



1 **Insights into Soil NO Emissions and the Contribution to Surface**
2 **Ozone Formation in China**

3

4 Ling Huang^{a,b}, Jiong Fang^a, Jiaqiang Liao^a, Yarwood Greg^c, Hui Chen^a, Yangjun Wang^a, Li Li^{a*}

5

6 ^aSchool of Environmental and Chemical Engineering, Shanghai University, Shanghai, 200444, China

7 ^bZhejiang Key Laboratory of Ecological and Environmental Big Data

8 ^cRamboll, Novato, California, 94945, USA

9

10 Corresponding author at: School of Environmental and Chemical Engineering, Shanghai University,
11 Shanghai 200444, China.

12 E-mail address: lily@shu.edu.cn (L. Li).

13

14 **Keywords:** Soil NO emissions; Ground-level ozone; BDSNP; OSAT

15

16 **Abstract.** Elevated ground-level ozone concentrations have emerged as a major
17 environmental issue in China. Nitrogen oxide (NO_x) is a key precursor to ozone formation.
18 Although control strategies aimed at reducing NO_x emissions from conventional combustion
19 sources are widely recognized, soil NO_x emissions (mainly as NO) due to microbial processes
20 have received little attention. The impact of soil NO emissions on ground-level ozone
21 concentration is yet to be evaluated. This study estimated soil NO emissions in China using
22 the Berkeley-Dalhousie soil NO_x parameterization (BDSNP) algorithm. A typical modeling
23 approach was used to quantify the contribution of soil NO emissions to surface ozone
24 concentration. The Brute-force method (BFM) and the Ozone Source Apportionment
25 Technology (OSAT) implemented in the Comprehensive Air Quality Model with extensions
26 (CAMx) were used. The total soil NO emissions in China for 2018 were estimated to be
27 1157.9 Gg N, with an uncertainty range of 715.7~1902.6 Gg N. Spatially, soil NO emissions
28 are mainly concentrated in Central China, North China, Northeast China, northern Yangtze
29 River Delta (YRD) and eastern Sichuan Basin, with distinct diurnal and monthly variations
30 that are mainly affected by temperature and the timing of fertilizer application. Both the BFM
31 and OSAT results indicate a substantial contribution of soil NO emissions to the maximum
32 daily 8-hour (MDA8) ozone concentrations by 8~12.5 μg/m³ on average for June 2018, with
33 the OSAT results consistently higher than BFM. The results also showed that soil NO
34 emissions led to a relative increase in ozone exceedance days by 10%~43.5% for selected
35 regions. Reducing soil NO emissions resulted in a general decrease in monthly MDA8 ozone
36 concentrations, and the magnitude of ozone reduction became more pronounced with
37 increasing reductions. However, even with complete reductions in soil NO emissions,



38 approximately 450.3 million people are still exposed to unhealthy ozone levels, necessitating
39 additional control policies. This study highlights the importance of soil NO emissions for
40 ground-level ozone concentrations and the potential of reducing NO emissions as a future
41 control strategy for ozone mitigation in China.

42 **1. Introduction**

43 With the substantial decrease in atmospheric fine particulate matter (PM_{2.5}) concentrations
44 during the past decade in China (Zhai et al., 2019; Xiao et al., 2020; Maji, 2020), ground-level
45 ozone (O₃) emerges as a simultaneously targeted air pollutant because high ozone
46 concentration increases respiratory and circulatory risks (Jerrett et al., 2009; Turner et al.,
47 2016; Malley et al., 2017) and reduces crop yields (Ainsworth et al., 2012; Feng et al., 2019;
48 Lin et al., 2018). A continuous increase in summertime surface ozone was observed across
49 China's nationwide monitoring network from 2013 to 2019, followed by an unprecedented
50 decline in 2020 (except for Sichuan Basin) (Sun et al., 2021), which is equally attributed to
51 meteorology and anthropogenic emissions reductions (Yin et al., 2021). As a secondary air
52 pollutant, ozone is generated by the photochemical oxidation of volatile organic compounds
53 (VOC) in the presence of nitrogen oxides (NO_x = NO + NO₂), both of which are considered
54 ozone precursors. The control strategies to mitigate ozone pollution in China focused on
55 reducing NO_x emissions at an early stage and started to stress the control of VOCs emissions
56 in recent years (e.g., the 2020 action plan on VOCs mitigation), including control of fugitive
57 emissions, stringent emissions standards, and substituting raw materials with low VOCs
58 content (Ecology, 2020). Ding et al. (2021) concluded that for North China Plain (NCP), a
59 region that experienced the most severe PM_{2.5} and ozone pollution in China, reductions in
60 NO_x emissions are essential regardless of VOC reduction.

61 Existing control strategies for NO_x emissions are almost exclusively targeted at combustion
62 sources, for example, power plants, industrial boilers, cement production, and vehicle
63 exhausts (Sun et al., 2018; Ding et al., 2017; Diao et al., 2018). However, NO_x emissions
64 from soils (mainly as NO), as a result of microbial processes (e.g., nitrification and
65 denitrification), could make up a substantial fraction of the total NO_x emissions (Hudman et
66 al., 2012; Lu et al., 2021), yet is often overlooked. In California, soil NO_x emissions in July
67 accounted for 40% of the state's total NO_x emissions and resulted in 23% of enhanced surface
68 ozone concentration (Sha et al., 2021). Romer et al. (2018) estimated that nearly half of the
69 increase in hot-day ozone concentration in a forested area of the rural southeastern United
70 States is attributable to the temperature-induced increases in NO_x emissions, mostly likely
71 due to soil microbes.

72 Soil NO emissions are affected by many factors, including nitrogen fertilizer application, soil
73 organic carbon content, soil temperature, humidity, and pH (Pilegaard, 2013; Bouwman et al.,



74 2002; Vinken et al., 2014; Yan et al., 2005). The amount of nitrogen fertilizer application in
75 China was estimated to account for one-third of the global nitrogen fertilizer application
76 (Heffer and Prud'homme, 2016), with most of the land under high nitrogen deposition (Liu et
77 al., 2013; Lü and Tian, 2007). Therefore, soil NO emissions in China are expected to be
78 significant, and their impacts on ozone pollution need to be systematically evaluated. So far,
79 only a limited number of studies have addressed this issue in China (Lu et al., 2021; Shen et
80 al., 2023; Wang et al., 2008; Wang et al., 2022). Lu et al. (2021) concluded that soil NO
81 significantly reduced the ozone sensitivity to anthropogenic emissions in NCP, therefore,
82 causing a so-called “emissions control penalty”. Wang et al. (2022) reported NO_x emissions
83 from cropland contributed 5.0% of the maximum daily 8h average ozone (MDA8 O₃) and
84 27.7% of NO₂ concentration in NCP. These studies focused solely on NCP, a region with
85 persistent O₃ pollution in warm seasons (Liu et al., 2020; Lu et al., 2020). The impact of soil
86 NO emissions on ozone concentrations over other regions, for example, the northern Yangtze
87 River Delta (YRD) and Sichuan Basin, where soil emissions are high (see Section 3.1) and
88 ozone pollution is also severe (Shen et al., 2022; Yang et al., 2021), has not been much
89 evaluated in details (Shen et al., 2023). In addition, the method employed in existing studies
90 to evaluate soil NO emissions on ozone concentration is the conventional “brute-force” zero-
91 out approach, which might be inappropriate given the strong nonlinearity of the ozone
92 chemistry (Clappier et al., 2017; Thunis et al., 2019).

93 With the deepening of emissions control measures for power, industrial and on-road sectors,
94 anthropogenic NO_x emissions from combustion sources have decreased at a much faster rate
95 (by 4.9% since 2012) than that from soil (fertilizer application decreases at a rate of 1.5%
96 since 2015, Fig. S1). Therefore, understanding the impacts of soil NO emissions on ground-
97 level ozone concentration, particularly considering the spatial heterogeneities over different
98 regions of China, is of great importance for formulating future ozone mitigation strategies. In
99 this study, soil NO emissions in China for 2018 were estimated based on a most recent soil
100 NO parameterization scheme with updated fertilizer data as input. The spatial and temporal
101 variations of soil NO emissions were described first. Uncertainties associated with estimation
102 of soil NO emissions were discussed. An integrated meteorology and air quality model was
103 applied to quantify the impact of soil NO emissions on surface ozone concentration based on
104 two different methods. Lastly, we evaluated the changes in ozone concentration and exposed
105 population under different emission scenarios to highlight the effectiveness of reducing soil
106 NO emissions as potential control policy. Our results provide insights into developing
107 effective emissions reduction strategies to mitigate the ozone pollution in China.



108 **2. Methodology**

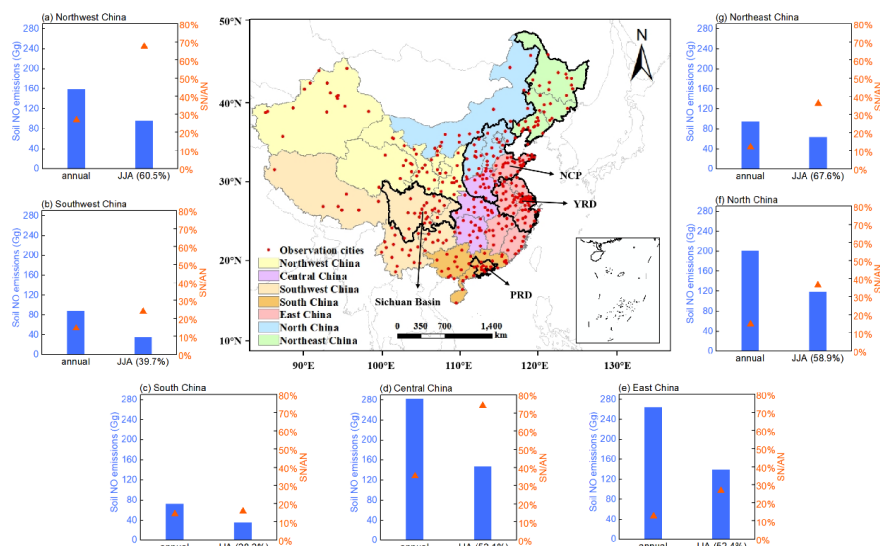
109 2.1. Estimation of soil NO emissions in China

110 Soil NO emissions were estimated based on the Berkeley-Dalhousie Soil NO_x
111 Parameterization (BDSNP) that is implemented in the Model of Emissions of Gases and
112 Aerosols from Nature (MEGAN) version 3.2 (<https://bai.ess.uci.edu/megan/data-and-code>,
113 accessed on September 1st, 2021). The BDSNP algorithm estimates the soil NO emissions by
114 adjusting a biome-specific NO emissions factor in response to various conditions, including
115 the soil temperature, soil moisture, precipitation-induced pulsing, and a canopy reduction
116 factor (Eq. 1):

$$NO_{\text{emission flux}} = A'_{\text{biome}}(N_{\text{avail}}) \times f(T) \times g(\theta) \times P(l_{\text{dry}}) \times CRF(LAI, Biome, Meteorology) \quad \text{Eq. 1}$$

117 where A'_{biome} is the biome-specific emission factor; $f(T)$ and $g(\theta)$ are the temperature and soil
118 moisture dependence functions, respectively; $P(l_{\text{dry}})$ represents the pulsed soil emissions due
119 to wetting of dry soils; and CRF describes the canopy reduction factor. The biome-specific
120 NO emissions factor A'_{biome} is a function of available nitrogen in the soil, which includes
121 fertilizer and wet/dry deposition of nitrogen species. Details concerning the BDSNP
122 parameterizations are described elsewhere (Hudman et al., 2012).

123 The default N fertilizer input data provided with the BDSNP algorithm is based on the
124 International Fertilizer Industry Association (IFA) fertilizer-use dataset for the year 2000
125 (Potter et al., 2010), which gives a number of 19.6 Tg N/a. In this study, we collected fertilizer
126 data from statistical yearbooks at the provincial level. The total amount of pure nitrogen
127 fertilizer (hereafter N fertilizer) applied in the year 2018 is 20.7 Tg N/a, which is similar
128 (5.6% higher) to IFA value. However, besides the N fertilizer, NPK compound fertilizer
129 (containing nitrogen (N), phosphorous (P), and potassium (K)) is being increasingly applied
130 in China. According to the statistical yearbook, the amount of N fertilizer applied decreased
131 from 23.5 Tg in 2010 to 20.7 Tg in 2018 (a relative reduction of 11.9%). In contrast, NPK
132 fertilizer increased from 18.0 in 2010 to 22.7 Tg in 2018 (a relative increase of 26.1%). We
133 assumed one-third of the NPK fertilizer is nitrogen (Liu, 2016); thus, the total amount of
134 nitrogen applied as fertilizer is 28.2 Tg N in 2018, which is 43.9% higher than the value from
135 Potter et al. (2010). We divided China into seven regions for emission analysis at regional
136 scale, namely Northeast China, North China, Central China, East China, South China,
137 Southwest China, and Northwest China, as indicated by different colors in Fig. 1 (see Table
138 S1 for the list of provinces in each region). At the regional level, the amount of total fertilizer
139 differs by as much as -147% to 69% from the default fertilizer.



140

141 Fig 1. Modeling domain and region definitions. Surrounding charts show the annual and
 142 summer (June-July-August, JJA) soil NO emissions and ratio of soil NO to anthropogenic
 143 NO_x emissions for each region.

144 2.2. Model configurations

145 A typical modeling approach was applied to evaluate the contribution of soil NO emissions to
 146 surface ozone concentration. The Weather Research and Forecasting (WRF) model (version
 147 4.0, <https://www.mmm.ucar.edu/wrf-model-general>, accessed on December 1st, 2021) and the
 148 Comprehensive Air Quality Model with Extension (CAMx, version 7.0,
 149 <http://www.camx.com/>, accessed on December 1st, 2021) were applied to simulate the
 150 meteorological fields and subsequent ozone concentrations. The model configuration is the
 151 same as our previous studies (Huang et al., 2021; Huang et al., 2022) and is briefly presented
 152 here. Anthropogenic emissions include the Multi-resolution Emission Inventory of China for
 153 2017 (MEIC, <http://www.meicmodel.org>, accessed on December 1st, 2021) and the 2010
 154 European Commission's Emissions Database for Global Atmospheric Research (EDGAR,
 155 <http://edgar.jrc.ec.europa.eu/index.php>, accessed on December 1st, 2021) for outside China.
 156 Biogenic emissions were calculated along with the soil NO emissions using MEGAN3.2.
 157 Open biomass burning emissions are adopted from the Fire INventory from NCAR version
 158 (FINN, version 1.5, <https://www.acom.ucar.edu/Data/fire/>) with MOZART speciation and
 159 converted to CAMx CB05 model species. The gaseous and aerosol modules used in CAMx
 160 include the CB05 chemical mechanism (Yarwood et al., 2010) and the CF module. The
 161 aqueous-phase chemistry is based on the updated mechanism of the Regional Acid Deposition
 162 Model (RADM) (Chang et al., 1987). A base case simulation was conducted for June 2018



163 when soil NO emissions reached maxima (Section 3.1) and ozone pollution was severe over
164 eastern China (Mao et al., 2020; Jiang et al., 2022). Base case model performances have been
165 evaluated in our previous studies (Huang et al., 2021; Huang et al., 2022). Here we evaluated
166 simulated ozone concentrations using the Pearson correlation coefficient (R), mean bias
167 (MB), root-mean-square error (RMSE), normalized mean bias (NMB), and normalized mean
168 error (NME) against hourly observed ozone concentrations for 365 cities in China. The
169 formula for each of the statistical metrics is given in Table S2. Observed hourly ozone
170 concentrations were obtained from the China National Environmental Monitoring Center.

171 2.3. Brute-force and OSAT

172 In this study, two methods were used to quantify the impact of soil NO emissions on surface
173 ozone concentration during the simulation period. The first is the conventional brute-force
174 method (BFM), which involves comparing the simulated ozone concentration between the
175 base case and a scenario case without soil NO emissions. The difference between these two
176 scenarios was considered to represent the contribution of soil NO emissions to ozone. The
177 second method applies the widely used Ozone Source Apportionment Technology (OSAT)
178 implemented in CAMx (Yarwood et al., 1996), with soil NO emissions being tagged as an
179 individual emission group. OSAT attributes ozone formation to NO_x or VOCs based on their
180 relative availability and apportions NO_x and VOCs emissions by source group/region
181 (Ramboll, 2021). In addition to soil NO emissions, anthropogenic and natural emissions
182 (including biogenic VOC emissions, lightning NO emissions, and open biomass burning)
183 were also tagged as individual emission groups.

184 3. Results and discussions

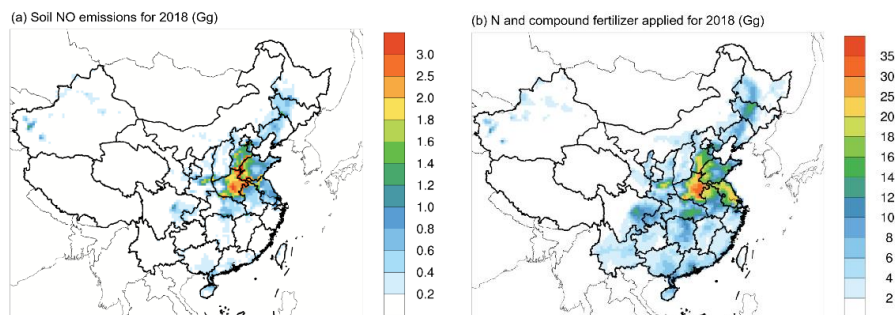
185 3.1. Soil NO emissions for 2018 in China

186 3.1.1. Spatial and temporal variations

187 National total soil NO emissions for 2018 is estimated to be 1157.9 Gg N, with an uncertainty
188 range of 715.7~1902.6 Gg N, which will be discussed more in Section 3.1.2. On an annual
189 scale, soil NO emissions accounted for 17.3% of the total anthropogenic NO_x emissions in
190 China for 2017 (based on MEIC inventory). This ratio varies from 12.0% to 35.3% at regional
191 scale. Unlike the anthropogenic NO_x emissions that concentrate over densely populated
192 regions (e.g., NCP, YRD), soil NO emissions are most abundant in Central China, particularly
193 Henan Province and nearby provinces, including Hebei and Shandong in the NCP, Jiangsu
194 and Anhui in northern YRD (Fig. 2a). Other hotspots of soil NO emissions include Northeast
195 China and the eastern part of the Sichuan Basin. As expected, the spatial distribution of soil
196 NO emissions closely mirrors that of the fertilizer application (Fig. 2b). Henan (located in
197 Central China), Shandong (NCP), and Hebei (NCP) are the top three provinces that have the



198 highest fertilizer application (together accounting for 24.1% of national totals in 2018) and
199 thus highest soil NO emissions (together accounting for 35.7%).

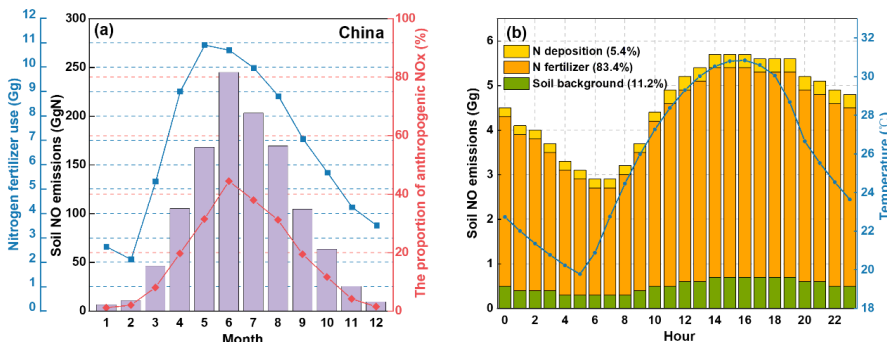


200 Fig 2. Spatial distribution of (a) soil NO emissions for 2018 and (b) N and compound
201 fertilizer applied for 2018.

202 In terms of the monthly variations, the total soil NO emissions show a unimodal pattern (as
203 shown in Fig. 3a with the highest emissions occurring in the summer months of June, July,
204 and August), except for South China and Southeast China (Fig. S2), where the peak emissions
205 occur in April or May. Soil NO emissions during the summer months account for 28.2%
206 (South China) to 67.6% (Northeast China) of the annual totals (Fig. 1 and Table S3). The
207 shape of monthly soil NO emissions is influenced by temperature and the timing of fertilizer
208 application. The BDSNP algorithm assumes that 75% of the annual fertilizer is applied over
209 the first month of the growing season, with the remaining 25% applied evenly throughout the
210 rest of the growing season. This assumption results in a significant amount of fertilizer being
211 applied from April to August (Fig. 3a). In contrast, anthropogenic NO_x emissions display
212 weaker monthly variations (Zheng et al., 2021). Consequently, the ratio of soil NO emissions
213 to anthropogenic NO_x (SN/AN) is much higher during the summer months. In regions such as
214 Central China and Northwest China, where soil NO emissions are high and anthropogenic
215 NO_x emissions are relatively low, SN/AN reaches 74.0% and 67.5% during the summer
216 months (Fig. 1 and Table S3). In East China and North China, where anthropogenic NO_x
217 emissions are high, SN/AN ranges from 26.3% to 46.0% during the summer months. These
218 findings are align with Chen et al. (2022), who reported that soil NO emissions made up 28%
219 of total NO_x (soil NO + anthropogenic NO_x) emissions in summer and could reach 50–90%
220 in isolated areas and suburbs. The substantial contribution of soil NO emissions during the
221 ozone pollution season implies a potentially significant impact on surface ozone
222 concentration. In terms of diurnal variations, soil NO emissions peak in the afternoon due to
223 diurnal temperature fluctuations. As illustrated by Fig. 3b, the average hourly soil NO
224 emissions over NCP for June 2018 closely follow the WRF simulated temperature changes.



225 The BDSNP algorithm identifies three sources of soil nitrogen: background, atmospheric
 226 nitrogen deposition, and fertilizer application, with the latter being the primary contributor. A
 227 decomposition analysis of soil NO emissions for NCP reveals that fertilizer application
 228 accounts for 83.4% of total NO soil emissions (Fig. 3b), while background and atmospheric
 229 nitrogen deposition only contribute for 11.2% and 5.4%, respectively. Thus, although soil NO
 230 emissions are generally considered a “natural” source (Galbally et al., 2008) and are not
 231 currently targeted in NO_x emission mitigation strategies, human fertilizer activities render soil
 232 NO emissions an anthropogenic source.



233 Fig. 3 (a) Monthly fertilizer (N + compound) applied and soil NO emissions in China and (b)
 234 hourly soil NO emissions for 2018 June in NCP and domain-averaged hourly 2-m temperature
 235 simulated by WRF.

236 3.1.2. Uncertainties associated with soil NO emission estimation

237 Although the BDSNP algorithm is considered more sophisticated than the old YL95
 238 algorithm, soil NO emissions are still subjected to large uncertainties. The first uncertainty
 239 comes from the amount of fertilizer application, which has been identified as the dominant
 240 contributor to soil NO emissions, as mentioned above. According to the global dataset (Potter
 241 et al., 2010), the amount of fertilizer applied is 19.6 Tg, which is comparable to the sum of
 242 nitrogen fertilizer for 2018 (20.7 Tg) obtained from provincial statistical yearbooks. However,
 243 compound fertilizer, usually with a nitrogen, phosphorus, and potassium ratio of 15: 15: 15,
 244 has been used more in China. Since 2016, the amount of nitrogen fertilizer has been
 245 decreasing annually at an average rate of 4.6%, while the amount of compound fertilizer has
 246 been increasing since 2010 at an average rate of 3.3%. The ratio of compound fertilizer to
 247 nitrogen fertilizer has increased from 76.4% in 2010 to 109.8% in 2018. Consequently, soil
 248 NO emissions may be largely underestimated if the compound fertilizer is not taken into
 249 account. Our calculation shows that if only nitrogen fertilizer is considered, the estimated
 250 total soil NO emissions are 805.2 Gg N a⁻¹ for 2018, which is comparable to the value (770
 251 Gg N a⁻¹ averaged during 2008-2017) reported by Lu et al. (2021), but 30.5% lower than that
 252 based on both nitrogen fertilizer and compound fertilizer. Regionally, this underestimation



253 ranges from 11.1%–41.5%, with a larger underestimation in Central China and East China
254 (Fig. S3).

255 Another major uncertainty in estimating soil NO emissions is the temperature dependence
256 factor $f(T)$ in Eq.1. According to the BDSNP scheme, soil NO emissions increase
257 exponentially with temperature between 0 and 30°C and reach a maximum when the
258 temperature exceeds 30°C. The default temperature dependence coefficient (i.e., k in Eq. S1)
259 follows the value used in the YL95 scheme, which is 0.103 ± 0.04 . However, as shown by
260 Table 3 in Yienger and Levy (1995), this value is the weighted average of values reported for
261 different land types, which shows a wide range from 0.040 to 0.189. Even for the same crop
262 type (e.g., corn), the value of k could be quite different (0.130 vs. 0.066). We conducted a
263 sensitivity analysis to examine the impact of varying the k value on estimated soil NO
264 emissions. When the k value decreases or increases by 20%, the estimated total soil NO
265 emissions change from 715.7 to 1902.6 Gg N/a, representing a relative difference of -
266 38.2~64.3% deviation from the default value (1157.9 Gg N/a). Using the default k value
267 would result in a large overestimation of simulated NO₂ concentrations over NCP and YRD
268 and underestimation over Northeast China (Fig. S4). According to the total sown areas of
269 farm crops reported in the provincial statistical yearbook, the primary crops grown in these
270 regions are wheat and corn, which have a relatively low k value (0.066~0.073). Therefore, we
271 adjusted k for NCP (reduced by 20%), YRD (reduced by 10%), and Northeast China
272 (increased by 10%). CAMx simulation results show that this adjustment would not
273 significantly affect the simulated MDA8 O₃ concentration but could reduce the NO₂ gap
274 between observation and simulation (Fig. S4-S5). Therefore, we applied this adjustment to
275 soil NO emissions in the following CAMx simulations.

276 The soil NO emissions estimated in this study were also compared with values reported by
277 existing studies based on either field measurement or model estimation (Table S4). Previous
278 studies report a wide range of soil NO emissions from 480 to 1375 Gg N and soil NO flux
279 ranging from 10 to 47.5 ng N m⁻² s⁻¹. The soil NO emissions estimated in our study are 1157.9
280 Gg N with the default k value and 951.9 Gg N with region-adjusted k value, which falls
281 within the upper range of previously reported values. The averaged soil NO flux over NCP in
282 June 2018 estimated in our study is 35.4 ng N m⁻² s⁻¹, which is within the range reported by
283 previous studies (12.9~40.0 ng N m⁻² s⁻¹).

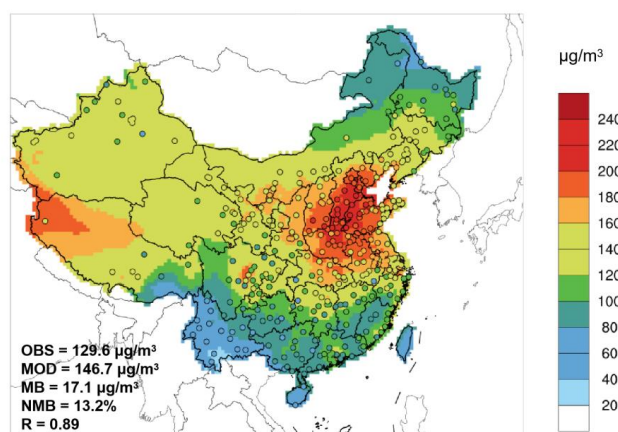
284 3.2. Contribution of soil NO emissions to ground-level ozone

285 3.2.1. Base case model evaluation

286 Fig. 4 shows the monthly averaged MDA8 ozone concentration simulated for June 2018 with
287 observed values presented on top. Overall the model well captured the spatial distribution of
288 MDA8 with a spatial correlation $R = 0.89$. Over the 365 cities in China, the simulated



289 monthly averaged MDA8 ozone concentration is $146.7 \pm 36.1 \mu\text{g}/\text{m}^3$, which is slightly higher
290 than the observed value of $129.6 \pm 37.6 \mu\text{g}/\text{m}^3$ (NMB = 13.2%). Regionally, model shows
291 better performance in Northeast China (MB = $2.4 \mu\text{g}/\text{m}^3$, NMB = 1.9%) and NCP (MB = 13.3
292 $\mu\text{g}/\text{m}^3$, NMB = 7.7%). Over-prediction is observed for Sichuan Basin and YRD (Table S5).



293

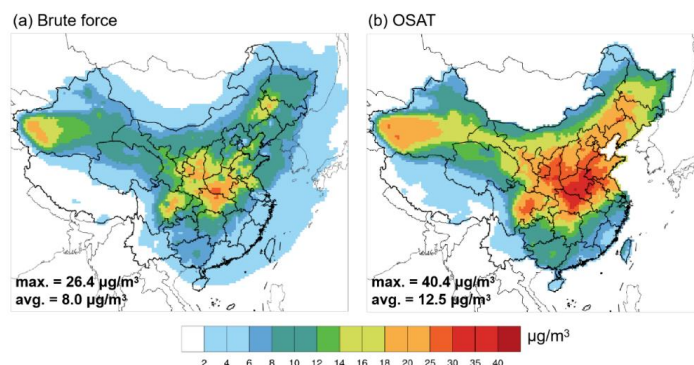
294 Fig 4. Comparison of simulated and observed values of MDA8 ozone in China in June 2018.

295 3.2.2. Impacts on regional ozone

296 To assess the contribution of soil NO emissions to surface ozone, both the brute-force method
297 (BFM) and the OSAT method were applied, and the results are shown in Fig. 5. Generally, the
298 two methods show consistent ozone contribution from soil NO emissions but with different
299 magnitudes. The BFM method shows widespread ozone enhancement due to soil NO
300 emissions with a spatial pattern that aligns with the distribution of soil NO emissions.
301 Substantial ozone enhancement is found over Central China, Sichuan Basin, northern YRD,
302 and eastern Northeast China. Maximum ozone enhancement (ΔMDA8) due to soil NO
303 emissions is $26.4 \mu\text{g}/\text{m}^3$ with a domain-average value of $8.0 \mu\text{g}/\text{m}^3$. For selected key regions,
304 the ozone contribution ranges from low to high: PRD ($3.8 \pm 1.1 \mu\text{g}/\text{m}^3$), YRD (8.7 ± 4.7
305 $\mu\text{g}/\text{m}^3$), Sichuan Basin ($9.1 \pm 0.9 \mu\text{g}/\text{m}^3$), Northeast ($9.3 \pm 3.0 \mu\text{g}/\text{m}^3$), and NCP (13.9 ± 4.4
306 $\mu\text{g}/\text{m}^3$), respectively. A similar spatial pattern is observed with the OSAT results, but the
307 magnitudes are much higher. Maximum ozone contribution by soil NO emissions reaches
308 $40.4 \mu\text{g}/\text{m}^3$ according to OSAT results, which is 53.0% higher than the brute force method.
309 The corresponding ozone contribution for each selected region is $6.7 \pm 1.2 \mu\text{g}/\text{m}^3$ (PRD), 13.5
310 $\pm 7.4 \mu\text{g}/\text{m}^3$ (Sichuan Basin), $14.5 \pm 4.9 \mu\text{g}/\text{m}^3$ (Northeast China), $16.2 \pm 7.8 \mu\text{g}/\text{m}^3$ (YRD)
311 and $25.7 \pm 5.3 \mu\text{g}/\text{m}^3$ (NCP). The scatter plots between BFM and OSAT results show good
312 correlations (Fig. S6, $R^2 = 0.78\text{--}0.97$), with OSAT results higher by 10%–61%. For YRD,
313 Sichuan Basin, and Northeast, the difference between the OSAT method and BFM increases



314 with the absolute ozone concentration (Fig. S7), while NCP shows the opposite trend. The
315 difference between the two methods reflects the nonlinear ozone response to NO_x emissions.
316 In addition to soil NO contribution, OSAT also gives ozone contributions from other source
317 groups, including anthropogenic emissions within China, boundary contribution, natural
318 emissions (e.g., biogenic emissions, open biomass burning, lightning NO_x), and emissions
319 outside China. The spatial distribution for each source category is presented in Fig. S8, and
320 the relative contribution for each selected region is shown in Fig. S9. Overall, boundary
321 transport (54.0%) and anthropogenic emissions (25.9%) contribute most to MDA8 ozone for
322 June 2018. Boundary contribution is high over the western and northern parts of China, while
323 the contribution from anthropogenic emissions is substantial over eastern China, where
324 anthropogenic emissions are extensive. On a national scale, soil NO emissions exhibit a
325 relative ozone contribution of 9.5%, and regionally this value ranges from 6% in PRD to 14%
326 in NCP.



327
328 Fig 5. Ozone contribution from soil NO emissions based on (a) brute force method and (b)
329 OSAT method.

330 We further evaluated the impact of soil NO emissions on the number of ozone exceedances
331 days (i.e., days with MDA8 O₃ higher than 160 µg/m³) during June 2018 based on the relative
332 response factor (RRF) method and results from the brute force method. The total number of
333 ozone exceedances days during June 2018 for the five selected regions ranged from 50 days
334 in PRD to 985 days in NCP (Table 1). The number of ozone exceedance days per city ranged
335 from 3.1 days in Sichuan Basin to 18.2 days in NCP, suggesting the severe ozone pollution in
336 June 2018 over NCP. RRF was first calculated for each city as the ratio of simulated ozone
337 concentration between the base case and the case with soil NO emissions excluded and
338 applied to the observed ozone concentrations to obtain adjusted ozone concentrations without
339 soil NO emissions. Soil NO emissions are estimated to lead to 121 ozone exceedance days in
340 NCP, followed by 84 days in the Northeast and 70 days in YRD, corresponding to a percent
341 change of 12.3%, 32.8%, and 10.5%, respectively. In Sichuan Basin, where soil NO emissions



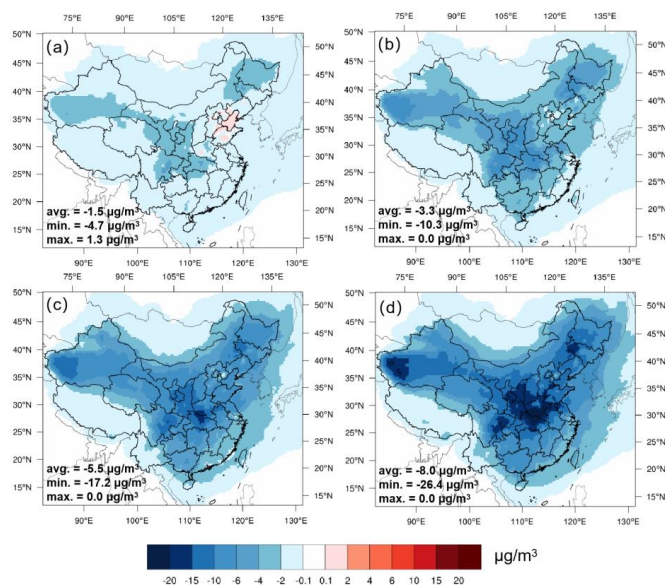
342 are also substantial, soil NO emissions contribute 30 ozone exceedances days, which accounts
 343 for 43.5% of the total ozone exceedances days. These results suggest the substantial
 344 contribution of soil NO emissions to the number of ozone pollution days over regions with
 345 high soil NO emissions.

346 **Table 1.** Number of ozone exceedances over selected regions during June 2018.

Region (No. of cities)	Number of ozone exceedance days (% of total days)	Δ ozone exceedances days when soil NO emissions are removed	% of total ozone exceedances days
NCP (54)	985 (60.8%)	-121	-12.3%
YRD (55)	666 (41.1%)	-70	-10.5%
PRD (9)	50 (18.5%)	-6	-12.0%
Sichuan Basin (22)	69 (10.5%)	-30	-43.5%
Northeast (37)	256 (23.1%)	-84	-32.8%

347 3.3. Ozone responses to reductions in soil NO emissions

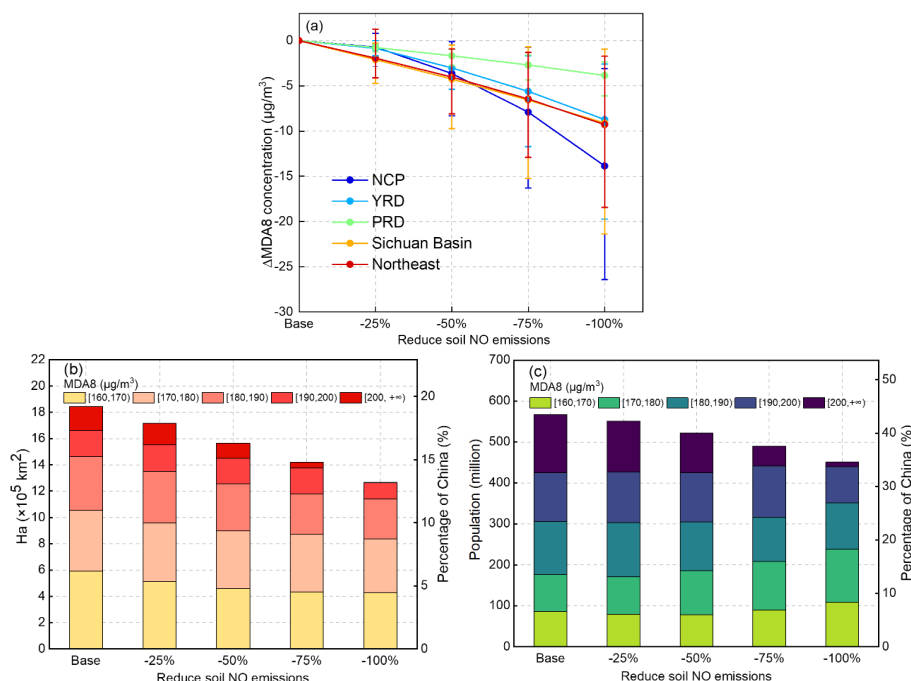
348 Current NO_x emission control policies primarily target combustion sources, such as power
 349 plants (Du et al., 2021) and on-road vehicles (Park et al., 2021). Nitrification inhibitors, such
 350 as dicyandiamide (DCD, C₂H₄N₄), have been found to be effective in reducing nitrogen loss,
 351 thereby reducing NO emissions from soil (Abalos et al., 2014). Studies have shown that using
 352 5% DCD with nitrogen fertilizer can reduce NO emissions by up to 70% (Xue et al., 2022). In
 353 light of this, it is important to evaluate the impact of reduced soil NO emissions on ozone
 354 concentration. To address this question, four sensitivity simulations were carried out for June
 355 2018, with soil NO emissions reduced by 25%, 50%, 75%, and 100% relative to the base
 356 case. As shown by Fig. 6, reducing soil NO emissions led to a general decrease in monthly
 357 MDA8 ozone concentration (Δ MDA8), with the magnitude of Δ MDA8 becoming more
 358 significant with the reduction ratio. With a 25% reduction in soil NO emissions, there was a
 359 widespread small decrease in monthly average MDA8 ozone concentration (Δ MDA8: -
 360 $1.5 \pm 0.9 \mu\text{g}/\text{m}^3$), except over NCP where ozone showed a slight increase (up to $1.3 \mu\text{g}/\text{m}^3$) in
 361 Shandong and Henan province. When soil NO emissions were cut by 50%, Δ MDA8 showed a
 362 ubiquitous decrease across entire China with an average Δ MDA8 of $-5.5 \mu\text{g}/\text{m}^3$. When soil
 363 NO emissions were removed entirely, the maximum Δ MDA8 could exceed $25 \mu\text{g}/\text{m}^3$ over
 364 central China, part of the Sichuan Basin, Northeast China, and Northeast China. Regions with
 365 strong ozone responses generally aligned with regions that also had high soil NO emissions.
 366 However, it should be noted that the ozone response to soil NO reductions not only depends
 367 on the magnitude of soil NO emissions but is also affected by (1) the local ozone formation
 368 regime that is further determined by the relative abundance of NO_x and VOCs, and (2)
 369 changes in transport of upwind ozone.



370

371 Fig 6. Spatial distribution of ΔMDA8 under (a) 25%, (b) 50%, (c) 75%, and (d) 100%
 372 reductions of soil NO emissions in June 2018.

373 Fig. 7a provides further details on the domain-averaged ΔMDA8 under different reduction
 374 scenarios for the five key regions. As expected, the ozone response in each region increased as the
 375 reduction in the soil NO emissions increased. NCP exhibited the strongest ozone responses to
 376 changes in soil NO emissions, with ΔMDA8 increasing from $-0.7 \pm 0.8 \mu\text{g}/\text{m}^3$ with 25% reductions
 377 to $-13.9 \pm 4.4 \mu\text{g}/\text{m}^3$ when all soil NO emissions were removed. YRD, Sichuan Basin, and
 378 Northeast China exhibit similar ozone responses when soil NO emissions are reduced. Under the
 379 25% scenario, ΔMDA8 ranged from -4.7 to $1.3 \mu\text{g}/\text{m}^3$ for these three regions; with 100% soil NO
 380 reductions, ΔMDA8 ranged from -21.4 to $-0.9 \mu\text{g}/\text{m}^3$. ΔMDA8 in PRD was relatively small. Even
 381 with a 100% reduction, the average ΔMDA8 in PRD was less than $5 \mu\text{g}/\text{m}^3$, which is associated
 382 with the small soil NO emissions in PRD. It is interesting to note that all regions except NCP
 383 exhibited an approximate linear ozone response to changes in soil NO emission reductions. NCP
 384 showed more significant ozone reductions as the reduction ratio increased, suggesting that NCP
 385 would gain more benefits with more aggressive reductions in soil NO emissions compared to other
 386 regions.



387 Fig 7. (a) Δ MDA8 concentrations in five key regions under different emission reduction
 388 scenarios (b) Area and (c) population exposed to different ozone levels under different soil
 389 NO emission reduction scenarios.

390 We evaluated the impact of different soil NO emission reduction scenarios on the area and
 391 population exposed to varying ozone levels. The results, presented in Fig. 7b and 7c, revealed
 392 a decrease in coverage and exposed population under high ozone concentrations as soil NO
 393 emissions decrease. The data presented in the plots are for grid cells with monthly MDA8
 394 ozone concentrations exceeding 160 $\mu\text{g}/\text{m}^3$. In the Base scenario, the estimated coverage of
 395 MDA8 ozone exceeding 160 $\mu\text{g}/\text{m}^3$ was $1.84 \times 10^6 \text{ km}^2$, equivalent to 19.2% of the national
 396 land area. The population exposed to ozone concentrations exceeding 160 $\mu\text{g}/\text{m}^3$ amounts to
 397 566.6 million, representing 43.4% of the entire population. The areas with extremely high
 398 ozone concentrations (MDA8 > 200 $\mu\text{g}/\text{m}^3$) account for 1.9% of the national land area, with a
 399 corresponding exposed population of 10.9%, indicating that densely populated areas
 400 experience higher ozone concentrations. When soil NO emissions are halved, there is a 15.2%
 401 reduction in the coverage of non-attainment areas and an 8.0% reduction in the total exposed
 402 population. If soil NO emissions are eliminated, the total area coverage and population
 403 exposed to MDA8 ozone concentrations exceeding 160 $\mu\text{g}/\text{m}^3$ would be $1.27 \times 10^6 \text{ km}^2$ and
 404 450.3 million, respectively, representing 13.2% and 34.5% of the total. Compared to the Base
 405 scenario, a 100% theoretical reduction in soil NO emissions leads to a 31.3% and 20.5%



406 reduction in the exposed area and population under high ozone concentration, respectively,
407 indicating substantial health benefits gained when soil NO emissions are mitigated.

408 Fig. S10-S11 displays similar area and population plots for selected key regions. The overall
409 trends for each sub-region are consistent. With 100% reductions in soil NO emissions, the
410 area with high ozone concentration decreased by 17.8%, 22.3%, 65.4%, and 100% for NCP,
411 YRD, Sichuan Basin, and Northeast. The corresponding values for the exposed population are
412 91.4%, 60.3%, 9.8%, and 0.0%. While the relative change is more significant in Sichuan
413 Basin and Northeast China, NCP and YRD gain more health benefits due to the significantly
414 higher total population for these two regions. However, it is worth noting that even with the
415 complete elimination of soil NO emissions, a total of 450.3 million people are still exposed to
416 ozone levels exceeding the national standard, necessitating additional control policies, such as
417 synergistic control of anthropogenic VOC emissions (Chen et al., 2022; Ding et al., 2021).

418 **4. Conclusions**

419 Soil NO emissions are non-negligible NO_x sources, particularly during summer. The
420 importance of soil NO emissions to ground-level ozone concentration in China is much less
421 evaluated than combustion NO_x emissions. In this study, the total national soil NO emissions
422 were estimated to be 1157.9 Gg N in 2018, with a spatial distribution closely following that of
423 fertilizer application. High soil NO emissions were mainly concentrated over Henan,
424 Shandong, and Hebei provinces, which differs from anthropogenic NO_x emissions. Distinct
425 diurnal and seasonal variations in soil NO emissions were simulated, mainly driven by the
426 changes in temperature as well as the timing of fertilizer application. Uncertainty analysis
427 reveals a range of 715.7~1902.6 Gg N of soil NO emissions that warrant further constraints
428 from observations.

429 Using two methods (BFM and OSAT), we evaluated the contribution of soil NO emissions to
430 ground-level ozone concentration for June 2018. Both methods suggest a substantial
431 contribution of soil NO emissions to MDA8 ozone concentrations by 8~12.5 µg/m³ on
432 average for June 2018, with the OSAT results consistently higher than BFM. Soil NO
433 emissions were shown to lead to a relative increase of ozone exceedances days by
434 10.0%~43.5% for selected regions. Reducing soil NO emissions could generally reduce the
435 ground-level ozone concentrations and populations exposed to unhealthy ozone levels
436 (MDA8 > 160 µg/m³), especially over NCP and YRD. With a 50% reduction in soil NO
437 emissions, the coverage of non-attainment areas and the population exposed to unhealthy
438 ozone levels decreased by 15.2% and 8.0%, respectively. However, even with the complete
439 removal of soil NO emissions, approximately 450.3 million populations are still exposed to
440 unhealthy ozone levels, necessitating additional control policies, such as synergistic control of
441 anthropogenic VOC emissions.



442 **Data availability.** Data will be made available on request.

443 **Author contributions.** **Ling Huang:** Conceptualization, Formal analysis, Writing – original
444 draft. **Jiong Fang:** Data curation, Formal analysis, Visualization. **Jiaqiang Liao:** Data
445 curation, Formal analysis, Visualization. **Yarwood Greg:** Writing – review & editing. **Chong**
446 **Han:** Writing – review & editing. **Du Bo:** Resources. **Hui Chen:** Writing – review & editing.
447 **Yangjun Wang:** Writing – review & editing. **Li Li:** Conceptualization, Supervision, Funding
448 acquisition.

449 **Competing interests.** The authors declare that they have no known competing financial
450 interests or personal relationships that could have appeared to influence the work reported in
451 this paper.

452 **Acknowledgments.** This study was financially sponsored by the National Natural Science
453 Foundation of China (grant No. 42005112, 42075144), the Open Funding of Zhejiang Key
454 Laboratory of Ecological and Environmental Big Data (No. EEBD-2022-06), the Shanghai
455 International Science and Technology Cooperation Fund (No.19230742500). This work is
456 supported by Shanghai Technical Service Center of Science and Engineering Computing,
457 Shanghai University.

458 **References**

- 459 Abalos, D., Jeffery, S., Sanz-Cobena, A., Guardia, G., and Vallejo, A.: Meta-analysis of the effect of
460 urease and nitrification inhibitors on crop productivity and nitrogen use efficiency, *Agriculture,*
461 *Ecosystems & Environment*, 189, 136-144, 2014.
- 462 Ainsworth, E. A., Yendrek, C. R., Sitch, S., Collins, W. J., and Emberson, L. D.: The effects of
463 tropospheric ozone on net primary productivity and implications for climate change, *Annual review of*
464 *plant biology*, 63, 637-661, 2012.
- 465 Bouwman, A., Boumans, L., and Batjes, N.: Modeling global annual N₂O and NO emissions from
466 fertilized fields, *Global Biogeochemical Cycles*, 16, 28-21-28-29, 2002.
- 467 Chang, J., Brost, R., Isaksen, I., Madronich, S., Middleton, P., Stockwell, W., and Walcek, C.: A three -
468 dimensional Eulerian acid deposition model: Physical concepts and formulation, *Journal of*
469 *Geophysical Research: Atmospheres*, 92, 14681-14700, 1987.
- 470 Chen, W., Guenther, A. B., Jia, S., Mao, J., Yan, F., Wang, X., and Shao, M.: Synergistic effects of
471 biogenic volatile organic compounds and soil nitric oxide emissions on summertime ozone formation in
472 China, *Science of The Total Environment*, 828, 154218, 2022.
- 473 Clappier, A., Belis, C. A., Pernigotti, D., and Thunis, P.: Source apportionment and sensitivity analysis:
474 two methodologies with two different purposes, *Geoscientific Model Development*, 10, 4245-4256,
475 2017.
- 476 Diao, B., Ding, L., Su, P., and Cheng, J.: The spatial-temporal characteristics and influential factors of
477 NO_x emissions in China: A spatial econometric analysis, *International journal of environmental*
478 *research and Public Health*, 15, 1405, 2018.
- 479 Ding, D., Xing, J., Wang, S., Dong, Z., Zhang, F., Liu, S., and Hao, J.: Optimization of a NO_x and
480 VOC cooperative control strategy based on clean air benefits, *Environmental Science & Technology*,
481 56, 739-749, 2021.



- 482 Ding, L., Liu, C., Chen, K., Huang, Y., and Diao, B.: Atmospheric pollution reduction effect and
483 regional predicament: An empirical analysis based on the Chinese provincial NO_x emissions, *Journal*
484 *of environmental management*, 196, 178-187, 2017.
- 485 Du, L., Zhao, H., Tang, H., Jiang, P., and Ma, W.: Analysis of the synergistic effects of air pollutant
486 emission reduction and carbon emissions at coal - fired power plants in China, *Environmental Progress*
487 *& Sustainable Energy*, 40, e13630, 2021.
- 488 The Chinese Ministry of Environmental and Ecology (MEE):. The volatile organic compound
489 management attack program in 2020 (in Chinese): (available
490 at:www.mee.gov.cn/xxgk/xxgk/xxgk03/202006/t20200624_785827.html), 2020.
- 491 Feng, Z., De Marco, A., Anav, A., Gualtieri, M., Sicard, P., Tian, H., Fornasier, F., Tao, F., Guo, A., and
492 Paoletti, E.: Economic losses due to ozone impacts on human health, forest productivity and crop yield
493 across China, *Environment international*, 131, 104966, 2019.
- 494 Galbally, I. E., Kirstine, W. V., Meyer, C., and Wang, Y. P.: Soil-atmosphere trace gas exchange in
495 semiarid and arid zones, *Journal of Environmental Quality*, 37, 599-607, 2008.
- 496 Heffer, P. and Prud'homme, M.: Global nitrogen fertilizer demand and supply: Trend, current level and
497 outlook, International Nitrogen Initiative Conference. Melbourne, Australia,
- 498 Huang, L., Kimura, Y., and Allen, D. T.: Assessing the impact of episodic flare emissions on ozone
499 formation in the Houston-Galveston-Brazoria area of Texas, *Science of The Total Environment*, 828,
500 154276, 2022.
- 501 Huang, L., Wang, Q., Wang, Y., Emery, C., Zhu, A., Zhu, Y., Yin, S., Yarwood, G., Zhang, K., and Li,
502 L.: Simulation of secondary organic aerosol over the Yangtze River Delta region: The impacts from the
503 emissions of intermediate volatility organic compounds and the SOA modeling framework,
504 *Atmospheric Environment*, 246, 118079, 2021.
- 505 Hudman, R., Moore, N., Mebust, A., Martin, R., Russell, A., Valin, L., and Cohen, R.: Steps towards a
506 mechanistic model of global soil nitric oxide emissions: implementation and space based-constraints,
507 *Atmospheric Chemistry and Physics*, 12, 7779-7795, 2012.
- 508 Jerrett, M., Burnett, R. T., Pope III, C. A., Ito, K., Thurston, G., Krewski, D., Shi, Y., Calle, E., and
509 Thun, M.: Long-term ozone exposure and mortality, *New England Journal of Medicine*, 360, 1085-
510 1095, 2009.
- 511 Jiang, Y., Wang, S., Xing, J., Zhao, B., Li, S., Chang, X., Zhang, S., and Dong, Z.: Ambient fine
512 particulate matter and ozone pollution in China: synergy in anthropogenic emissions and atmospheric
513 processes, *Environmental Research Letters*, 17, 123001, 2022.
- 514 Lin, Y., Jiang, F., Zhao, J., Zhu, G., He, X., Ma, X., Li, S., Sabel, C. E., and Wang, H.: Impacts of O₃
515 on premature mortality and crop yield loss across China, *Atmospheric Environment*, 194, 41-47, 2018.
- 516 Liu, H. Z., Qingqing Liu: Distribution of Fertilizer Application and Its Environmental Risk in Different
517 Provinces of China, *Chemical Management*, 174-174, 2016.
- 518 Liu, P., Song, H., Wang, T., Wang, F., Li, X., Miao, C., and Zhao, H.: Effects of meteorological
519 conditions and anthropogenic precursors on ground-level ozone concentrations in Chinese cities,
520 *Environmental Pollution*, 262, 114366, 2020.
- 521 Liu, X., Zhang, Y., Han, W., Tang, A., Shen, J., Cui, Z., Vitousek, P., Erisman, J. W., Goulding, K., and
522 Christie, P.: Enhanced nitrogen deposition over China, *Nature*, 494, 459-462, 2013.
- 523 Lü, C. and Tian, H.: Spatial and temporal patterns of nitrogen deposition in China: synthesis of
524 observational data, *Journal of Geophysical Research: Atmospheres*, 112, 2007.



- 525 Lu, X., Zhang, L., Wang, X., Gao, M., Li, K., Zhang, Y., Yue, X., and Zhang, Y.: Rapid increases in
526 warm-season surface ozone and resulting health impact in China since 2013, *Environmental Science &*
527 *Technology Letters*, 7, 240-247, 2020.
- 528 Lu, X., Ye, X., Zhou, M., Zhao, Y., Weng, H., Kong, H., Li, K., Gao, M., Zheng, B., and Lin, J.: The
529 underappreciated role of agricultural soil nitrogen oxide emissions in ozone pollution regulation in
530 North China, *Nature communications*, 12, 5021, 2021.
- 531 Maji, K. J.: Substantial changes in PM_{2.5} pollution and corresponding premature deaths across China
532 during 2015–2019: A model prospective, *Science of the Total Environment*, 729, 138838, 2020.
- 533 Malley, C. S., Henze, D. K., Kuylentierna, J. C., Vallack, H. W., Davila, Y., Anenberg, S. C., Turner,
534 M. C., and Ashmore, M. R.: Updated global estimates of respiratory mortality in adults ≥ 30 years of
535 age attributable to long-term ozone exposure, *Environmental health perspectives*, 125, 087021, 2017.
- 536 Mao, J., Wang, L., Lu, C., Liu, J., Li, M., Tang, G., Ji, D., Zhang, N., and Wang, Y.: Meteorological
537 mechanism for a large-scale persistent severe ozone pollution event over eastern China in 2017, *Journal*
538 *of Environmental Sciences*, 92, 187-199, 2020.
- 539 Park, J., Shin, M., Lee, J., and Lee, J.: Estimating the effectiveness of vehicle emission regulations for
540 reducing NO_x from light-duty vehicles in Korea using on-road measurements, *Science of The Total*
541 *Environment*, 767, 144250, 2021.
- 542 Pilegaard, K.: Processes regulating nitric oxide emissions from soils, *Philosophical Transactions of the*
543 *Royal Society B: Biological Sciences*, 368, 20130126, 2013.
- 544 Potter, P., Ramankutty, N., Bennett, E. M., and Donner, S. D.: Characterizing the spatial patterns of
545 global fertilizer application and manure production, *Earth interactions*, 14, 1-22, 2010.
- 546 Ramboll: User's Guide: Comprehensive Air quality Model with extensions, Version 7.1., 2021.
- 547 Romer, P. S., Duffey, K. C., Wooldridge, P. J., Edgerton, E., Baumann, K., Feiner, P. A., Miller, D. O.,
548 Brune, W. H., Koss, A. R., and De Gouw, J. A.: Effects of temperature-dependent NO_x emissions on
549 continental ozone production, *Atmospheric Chemistry and Physics*, 18, 2601-2614, 2018.
- 550 Sha, T., Ma, X., Zhang, H., Janecek, N., Wang, Y., Wang, Y., Castro García, L., Jenerette, G. D., and
551 Wang, J.: Impacts of Soil NO_x Emission on O₃ Air Quality in Rural California, *Environmental science*
552 *& technology*, 55, 7113-7122, 2021.
- 553 Shen, L., Liu, J., Zhao, T., Xu, X., Han, H., Wang, H., and Shu, Z.: Atmospheric transport drives
554 regional interactions of ozone pollution in China, *Science of The Total Environment*, 830, 154634,
555 2022.
- 556 Shen, Y., Xiao, Z., Wang, Y., Xiao, W., Yao, L., and Zhou, C.: Impacts of agricultural soil NO_x
557 emissions on O₃ over Mainland China, *Journal of Geophysical Research: Atmospheres*,
558 e2022JD037986, 2023.
- 559 Sun, W., Shao, M., Granier, C., Liu, Y., Ye, C., and Zheng, J.: Long - term trends of Anthropogenic
560 SO₂, NO_x, CO, and NMVOCs emissions in China, *Earth's Future*, 6, 1112-1133, 2018.
- 561 Sun, Y., Yin, H., Lu, X., Notholt, J., Palm, M., Liu, C., Tian, Y., and Zheng, B.: The drivers and health
562 risks of unexpected surface ozone enhancements over the Sichuan Basin, China, in 2020, *Atmospheric*
563 *Chemistry and Physics*, 21, 18589-18608, 2021.
- 564 Thunis, P., Clappier, A., Tarrasón, L., Cuvelier, C., Monteiro, A., Pisoni, E., Wesseling, J., Belis, C.,
565 Pirovano, G., and Janssen, S.: Source apportionment to support air quality planning: Strengths and
566 weaknesses of existing approaches, *Environment International*, 130, 104825, 2019.



567 Turner, M. C., Jerrett, M., Pope III, C. A., Krewski, D., Gapstur, S. M., Diver, W. R., Beckerman, B. S.,
568 Marshall, J. D., Su, J., and Crouse, D. L.: Long-term ozone exposure and mortality in a large
569 prospective study, *American journal of respiratory and critical care medicine*, 193, 1134-1142, 2016.
570 Vinken, G., Boersma, K., Maasackers, J., Adon, M., and Martin, R.: Worldwide biogenic soil NO_x
571 emissions inferred from OMI NO₂ observations, *Atmospheric Chemistry and Physics*, 14, 10363-
572 10381, 2014.
573 Wang, Q. g., Han, Z., Wang, T., and Zhang, R.: Impacts of biogenic emissions of VOC and NO_x on
574 tropospheric ozone during summertime in eastern China, *Science of the total environment*, 395, 41-49,
575 2008.
576 Wang, R., Bei, N., Wu, J., Li, X., Liu, S., Yu, J., Jiang, Q., Tie, X., and Li, G.: Cropland nitrogen
577 dioxide emissions and effects on the ozone pollution in the North China plain, *Environmental
578 Pollution*, 294, 118617, 2022.
579 Xiao, Q., Geng, G., Liang, F., Wang, X., Lv, Z., Lei, Y., Huang, X., Zhang, Q., Liu, Y., and He, K.:
580 Changes in spatial patterns of PM_{2.5} pollution in China 2000–2018: Impact of clean air policies,
581 *Environment international*, 141, 105776, 2020.
582 Xue, C., Ye, C., Liu, P., Zhang, C., Su, H., Bao, F., Cheng, Y., Catoire, V., Ma, Z., and Zhao, X.: Strong
583 HONO Emissions from Fertilized Soil in the North China Plain 4 Driven by Nitrification and Water
584 Evaporation, 2022.
585 Yan, X., Ohara, T., and Akimoto, H.: Statistical modeling of global soil NO_x emissions, *Global
586 Biogeochemical Cycles*, 19, 2005.
587 Yang, X., Wu, K., Lu, Y., Wang, S., Qiao, Y., Zhang, X., Wang, Y., Wang, H., Liu, Z., and Liu, Y.:
588 Origin of regional springtime ozone episodes in the Sichuan Basin, China: role of synoptic forcing and
589 regional transport, *Environmental Pollution*, 278, 116845, 2021.
590 Yarwood, G., Morris, R., Yocke, M., Hogo, H., and Chico, T.: Development of a methodology for
591 source apportionment of ozone concentration estimates from a photochemical grid model, AIR &
592 WASTE MANAGEMENT ASSOCIATION, PITTSBURGH, PA 15222(USA).[np]. 1996.
593 Yarwood, G., Jung, J., Whitten, G. Z., Heo, G., Mellberg, J., and Estes, M.: Updates to the Carbon
594 Bond mechanism for version 6 (CB6), 9th Annual CMAS Conference, Chapel Hill, NC, 11-13,
595 Yienger, J. and Levy, H.: Empirical model of global soil - biogenic NO_x emissions, *Journal of
596 Geophysical Research: Atmospheres*, 100, 11447-11464, 1995.
597 Yin, H., Lu, X., Sun, Y., Li, K., Gao, M., Zheng, B., and Liu, C.: Unprecedented decline in summertime
598 surface ozone over eastern China in 2020 comparably attributable to anthropogenic emission reductions
599 and meteorology, *Environmental Research Letters*, 16, 124069, 2021.
600 Zhai, S., Jacob, D. J., Wang, X., Shen, L., Li, K., Zhang, Y., Gui, K., Zhao, T., and Liao, H.: Fine
601 particulate matter (PM_{2.5}) trends in China, 2013–2018: separating contributions from anthropogenic
602 emissions and meteorology, *Atmospheric Chemistry and Physics*, 19, 11031-11041, 2019.
603 Zheng, B., Zhang, Q., Geng, G., Chen, C., Shi, Q., Cui, M., Lei, Y., and He, K.: Changes in China's
604 anthropogenic emissions and air quality during the COVID-19 pandemic in 2020, *Earth System
605 Science Data*, 13, 2895-2907, 2021.
606